PLASMA FLOW SUPPRESSION IN THE OPEN MAGNETIC TRAPS BY THE HELICAL MIRROR

A.V. SUDNIKOV
Budker Institute of Nuclear Physics
Novosibirsk, Russian Federation
Email: A.V.Sudnikov@inp.nsk.su

A.D. BEKLEMISHEV[1], A.V. BURDAKOV[1], I.A. IVANOV[1], A.A. INZHEVATKINA[1], M.V LARICHKIN[2], K.A. LOMOV[2], V.F. SKLYAROV[1], V.V. POSTUPAEV[1], M.S. TOLKACHEV[2], V.O. USTYUZHANIN[2]
[1] Budker Institute of Nuclear Physics
[2] Novosibirsk State University
Novosibirsk, Russian Federation

Abstract

The paper presents experimental results from the SMOLA device that is the first facility with a helical mirror section of the magnetic field. This device is built in the Budker Institute of Nuclear Physics for the verification of the helical mirror confinement idea that is the recently introduced technique of the active control of axial losses from a confinement zone. Theory predicts that with rotating plasma, a helical mirror will provide suppression of the axial plasma flow and, simultaneously, density pinching to the axis. Experiments demonstrated the increase in plasma density between the simple mirror and the helical one by the factor of 1.6 compared to the straight magnetic system. The integral flux from the transport section drops below the detectable level. The effective mirror ratio of the helical section was $R_{eff} > 10$. Particle flux returning from the distant part of the helical mirror towards the confinement zone was observed. At high corrugation ratio the flux direction is different on the axis and on the periphery of the plasma in the helical section. All fluxes scale linearly on the plasma density, even if the mean free path of the ion is comparable to the length of the helical section.

1. INTRODUCTION

The challenge of creation of an open trap with the reactor-grade plasma is achievable if such trap will use specialized sections of the magnetic system for suppression of particle and energy losses along the magnetic field. The project of the next generation of the open trap GDMT includes the central gas-dynamic cell (0.3–2 T at midplane, 12–20 T in mirrors) and improved axial confinement [1]. Basic method of suppression of the axial flux for the project is multiple-mirror confinement [2], which can provide effective mirror ratio of the order of 100 and gives fusion gain appropriate for the hybrid reactor and, in optimistic case, for pure fusion.

Another way is the helical mirror confinement [3]. That proposal renewed an idea of a plasma control by moving magnetic mirrors. Modulation of the guiding magnetic field travelling in the laboratory reference frame have limitations on corrugation depth and possibility of utilizing superconducting coils [4]. The idea of the helical mirror considers a flow of a rotating plasma through a linear static magnetic system with helical corrugation that looks like a straightened stellarator. Periodical variations of the magnetic field moving upstream in plasma's reference frame transfer momentum to trapped particles and lead to plasma pumping towards the central trap. The helical mirror should have two improvements over the classical multiple-mirrors: the exponential law of the confinement improvement with the system length and the radial pinch of the ions that can counteract the diffusive broadening of the plasma stream [5, 6].

Concept exploration helical mirror «SMOLA» was put in operation in the end of 2017 in BINP [7, 8]. Plasma flux suppression by the helical sections was demonstrated in the first experimental campaign, integral suppression ratio of 2–2.5 was achieved [9]. An increase of the suppression ratio with the increase of the magnetic field, corrugation ratio and plasma rotation velocity was demonstrated [10]. This paper presents the latest experimental results on the plasma flows in the helical mirror in a broad range of the plasma densities at high rotation velocity and high corrugation ratio.

2. EXPERIMENTAL SET-UP

Layout of the SMOLA helical mirror is presented on the Fig. 1. Plasma was generated in the source with the magnetically insulated heated LaB_6 cathode [11]. Then the plasma was injected into the compact mirror trap in the entrance tank. In the discussed experiments the mirrors of this trap were asymmetric with mirror ratios $R \approx 8$ and $R \approx 3$ on the different sides of the trap. Plasma flows from the entrance tank to the transport section. This section has two independent magnetic systems, a solenoid for a straight field and a bispiral helical winding that

forms helical magnetic mirrors. The spiral has $N = 12$ periods of the corrugation. The last part of the device is the exit expander that contains an exit limiter and a radially segmented plasma receiver endplates. Detailed description of the device can be found in [8].

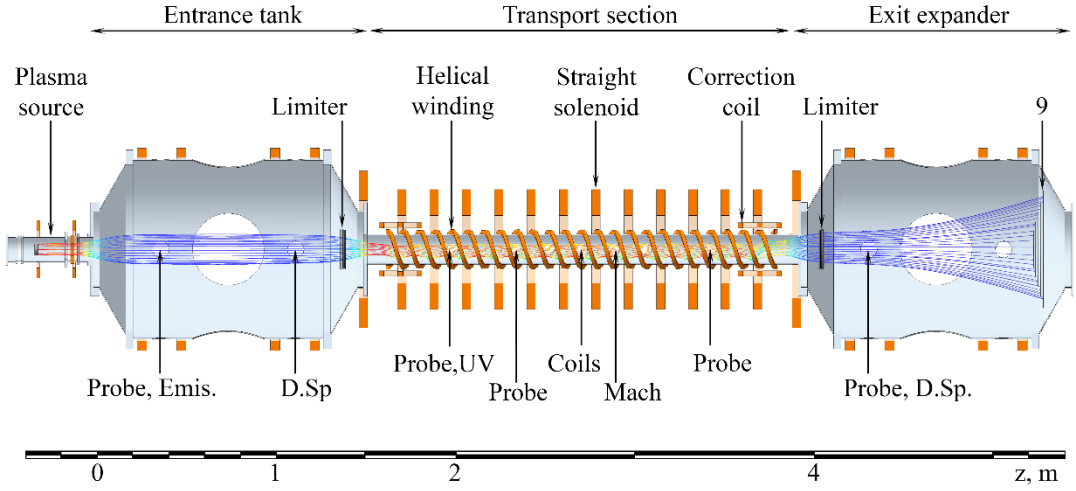

FIG. 1. Layout of the SMOLA helical mirror. Positions of the main diagnostics are indicated below the scheme. Probe: double electrostatic probes, Emis.: Emissive probe, D.Sp: Doppler spectroscopy, UV: photodiode detector of the vacuum UV radiation, Coils: 12-channel set of Mirnov coils, Mach: planar Mach probe.

Distribution of the guiding magnetic field is shown on the Fig. 2. Later in this paper the magnetic configuration will be described by the guiding magnetic field in the transport section, all other magnetic fields vary proportionally. Another parameter is the mean corrugation depth R_{mean}, which is the ratio of the maximal and the minimal magnetic field along the field line within the transport section averaged over the plasma cross-section. In the discussed experiments the magnetic field was in the range $B_z = 40–100$ mT, and the mean corrugation depth was in the range $R_{mean} = 1–1.7$, where 1 stands for the straight field without the helical component.

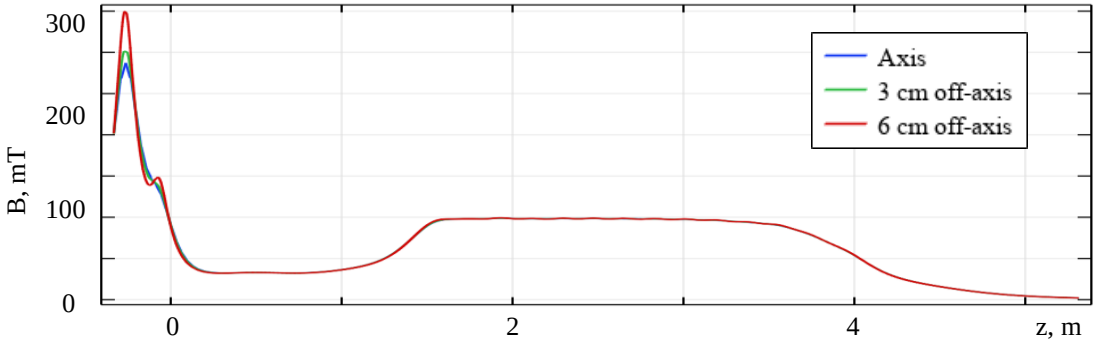

FIG. 2. Guiding magnetic field profiles for different radii.

The plasma density in the central cell was in the range $n = (1–4)\cdot10^{18}$ m^{-3}, temperatures were $T_i \approx 4$ eV and $T_e \approx 30$ eV. These values correspond to the mean free path of an ion in the entrance tank with respect to the Coulomb scattering $\lambda = 0.2–0.8$ m. The density in the transport section is by the factor 1.5–2 lower, thus giving the ratio of the mean free path to the period of the helical corrugation $\lambda/h \sim 1$ on the high density bound and $\lambda/h \sim N$ on the low density bound. Plasma rotation velocity in the discussed experiments was $\omega = (1–1.2)\cdot10^6$ s^{-1} in the entrance tank and $\omega = (0.6–0.8)\cdot10^6$ s^{-1} in the exit expander.

The main diagnostic for the plasma flux densities was the set of the radially movable electrostatic probes distributed over the length of the device. This set includes 1 double probe measuring I-V characteristic ($z = 0.4$ m), 4 double probes in ion saturation regime, 1 emissive probe and 1 Mach probe which has two planar double probes sputtered on the opposite sides of the dielectric plate. The Mach probe was oriented normally to

the guiding magnetic field, so the upstream side collects only the ions with $v_z > 0$ and the downstream side collects only ions with $v_z < 0$. Two Doppler spectrometers with the spatial resolution and the set of the Mirnov coils were used to measure plasma rotation [12]. Typical experimental waveforms are shown on Fig. 3.

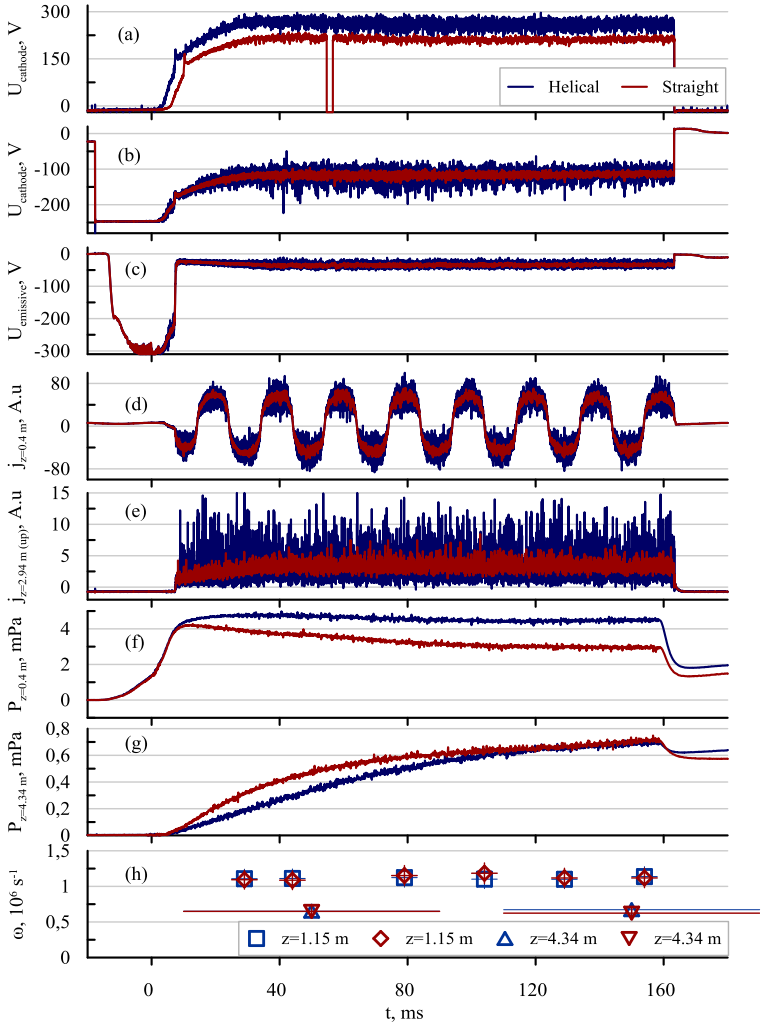

FIG. 3. Typical waveforms of the plasma parameters in the discharges with straight (red curves) and helically corrugated (blue curves) magnetic configurations. Time t=0 corresponds to the discharge initiation. From top to bottom: (a) the discharge current; (b) the voltage between the anode and the cathode of the plasma gun; (c) the potential of the emissive probe at z=0.4 m; (d) the current of the double probe at z=0.4 m (I-V curve measurement); (e) the current of the upstream side of the Mach probe (ion saturation current measurement); (f) the neutral hydrogen pressure at z=0.4 m; (g) the neutral hydrogen pressure at z=4.34 m, (h) plasma rotation velocity at z=1.15 m and z=4.34 m..

3. EXPERIMENTAL RESULTS

This experimental campaign was focused on the thorough investigation of the axial plasma fluxes in the transport section. For that reason, the detailed radial profiles of the plasma parameters were measured. In these experiments, we varied the guide magnetic field (B_z = 40–100 mT), the mean corrugation ratio (R_{mean} = 1–1.7) and the flux of the neutral hydrogen from the gas feeding system into the plasma source. The last parameter determines the density of the generated plasma. Typical radial profiles of the main plasma parameters in the entrance tank and the transport section are shown on Fig. 4. These profiles were fitted by the analytical function. The following form returned the best fit in the entrance tank and in the entrance of the transport section:

$$f(r) = a_1 \exp\left(-\left(\frac{r-r_0}{r_1}\right)^4\right) + a_2 \exp\left(-\left(\frac{r-r_0}{r_2}\right)^2\right)$$

The sum of the shifted Gaussian functions provided better fit in the other parts of the plasma stream:

$$f(r) = a_1 \exp\left(-\left(\frac{r-r_0}{r_1}\right)^2\right) + a_2 \exp\left(-\left(\frac{r-r_0}{r_2} - \Delta\right)^2\right)$$

We integrated these fitted functions across the cross-section in assumption of the azimuthal symmetry of the plasma parameters about the center of the fitted function r_0.

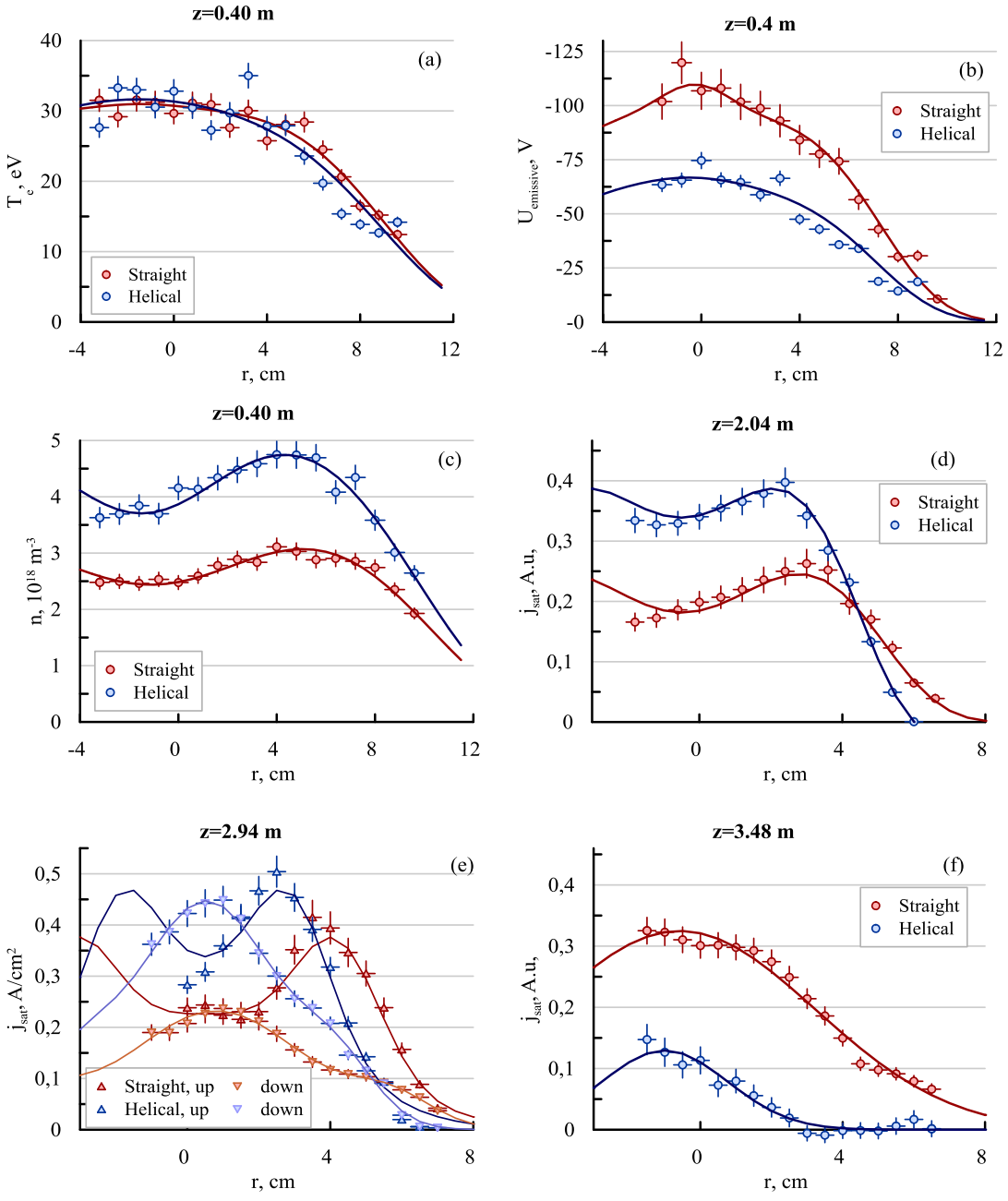

FIG. 4. Sample radial profiles. Dots show experimental data, lines are fitting functions. Helical field corresponds to R_{mean}=1.55. From left to right, from top to bottom: (a) electron temperature; (b) plasma potential; (c) plasma density in the entrance tank; ion saturation flux density (d) at the entrance of the transport section; (e) in the middle of the transport section on the upstream and downstream sides of the Mach probe; (f) at the exit of the transport section.

One can observe the rise of the maximal plasma flux density and the radial contraction of the plasma column with the activation of the helical field. The amplitude of the plasma flux and the width of the plasma stream at

the exit from the transport section decreases significantly. One more notable effect is the significant rise of the particle flux density on the downstream side of the Mach probe. In the central region the flux density returning back to the entrance tank becomes higher than the flux density going in the normal direction (Fig. 4 e,f).

The dependencies of the integrated fluxes on the relative amplitude of the helical component of the magnetic field are shown on Fig. 5. The clearest evidence of the helical mirror effect is 1.6-fold rise in the number of the particles confined in the entrance tank between the simple mirror and the helical one (Fig. 5 a). It agrees well with the significant drop in the particle flux at the exit from the transport section (Fig. 5 f). The particle flux decreases gradually with the increase of the corrugation ratio. At the high corrugation ratio (R_{mean} = 1.7) the integral flux from the transport section drops below the detectable level.

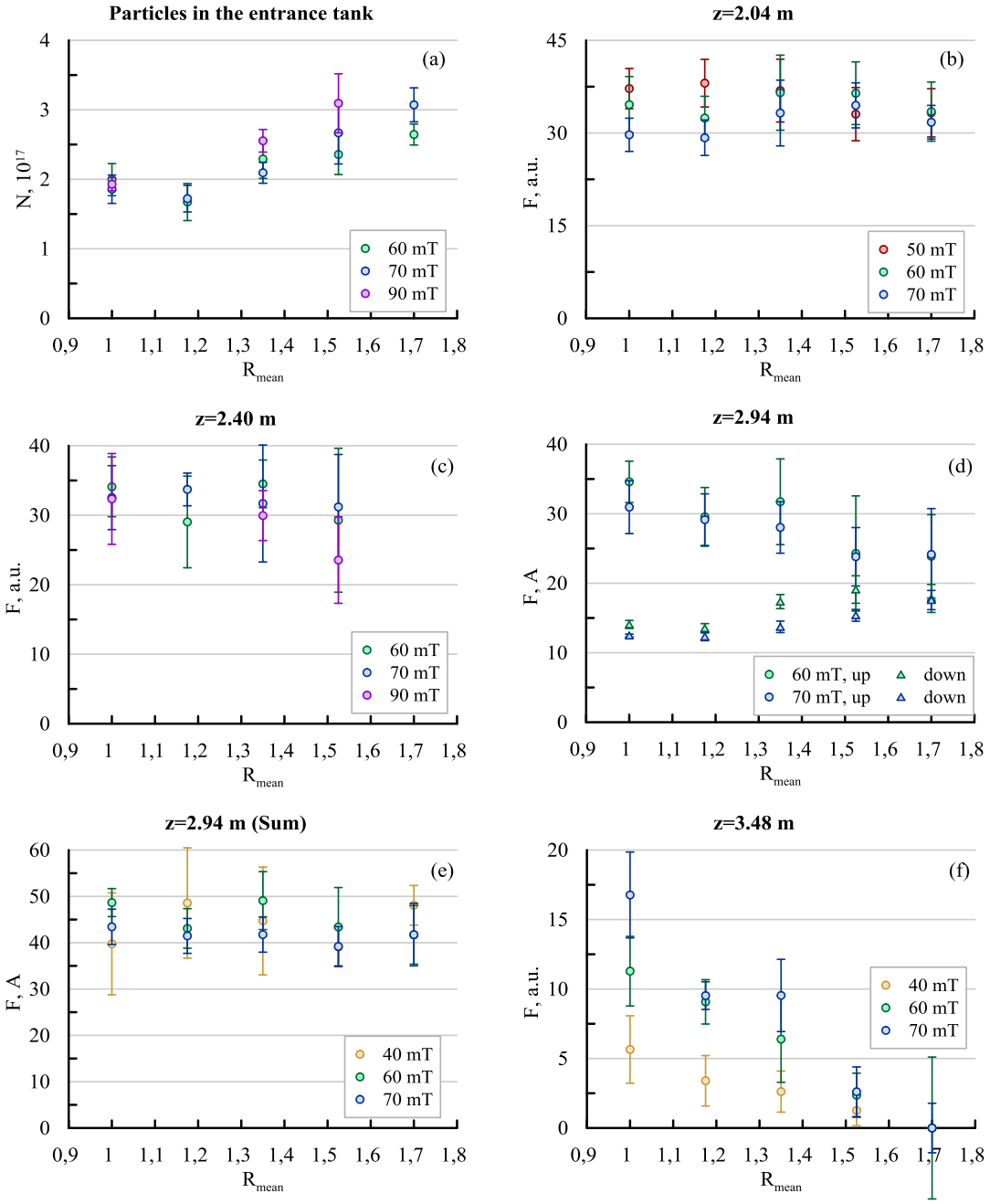

FIG. 5. Dependence of the particle number and integral flux density on the mean corrugation ratio. From left to right, from top to bottom: (a) number of particles in the entrance tank; plasma flux (b) at the entrance of the transport section; (c) in the middle of the transport section; (d) on the upstream and downstream sides of the Mach probe; (e) on the both sides of the Mach probe; (f) at the exit of the transport section.

In contrast, the particle flux detected by the double probes in the entrance half of the transport section changes insignificantly with the corrugation ratio (Fig. 5 b,c). More detailed information on the particle flux was obtained by the Mach probe installed close to the center of the transport section (Fig. 5 d). The integral particle flux from the plasma source towards the exit from the transport section gradually decreases, while the return flux increases by the factor of 1.5. At highest achievable corrugation ratio the difference between the outcoming and return fluxes becomes lower than the corresponding confidence interval. At the same time, the total flux on the both sides of the Mach probe stay almost unchanged (Fig. 5 e).

The dependence of the integral particle fluxes on the plasma density (Fig. 6) was measured at guide magnetic field B_z = 70mT and mean corrugation ratio R_{mean} = 1.35. We should note (see Fig. 5) that at such corrugation ratio the effect of the helical confinement is not very sharp. All fluxes, including the return flux on the downstream side of the Mach probe, scale linearly with the gas feeding of the plasma source. No significant difference in the densities of the forward and return fluxes normalized by the flux density in the entrance of the transport section was observed. Return flux is observed even at low classical collisionality.

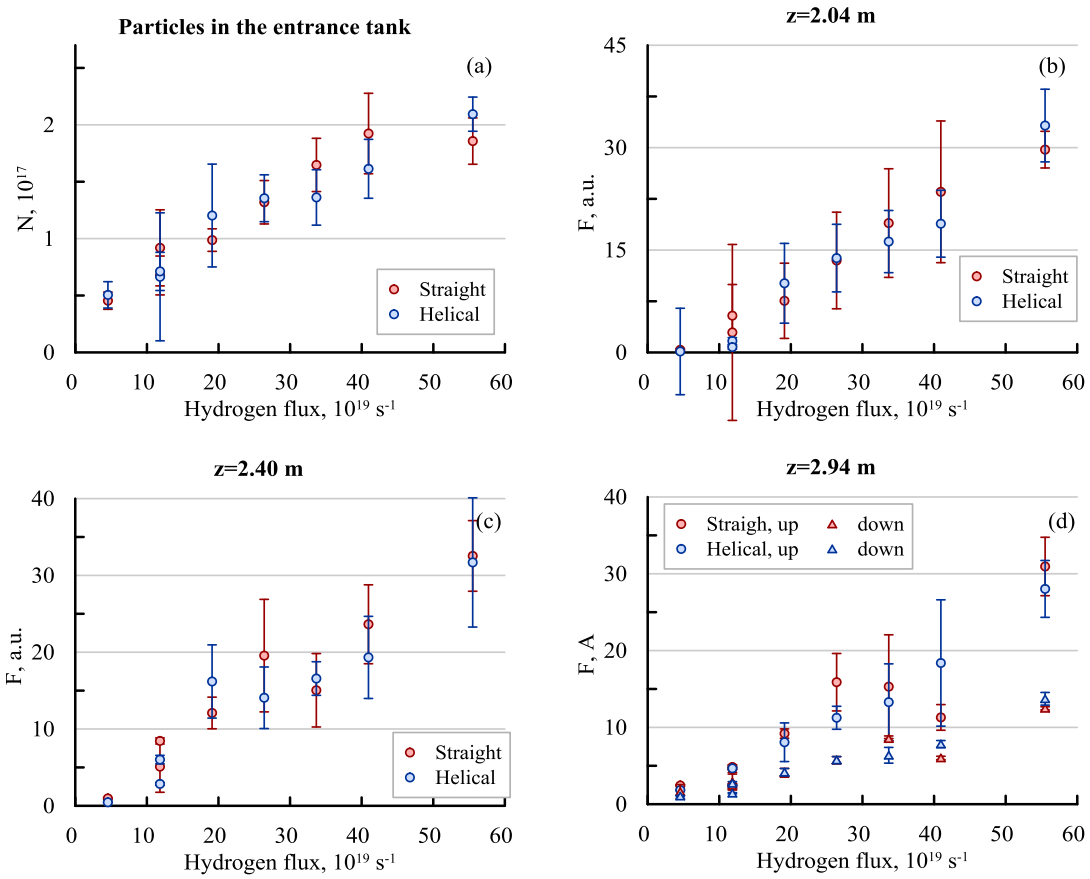

FIG. 6. Dependence of the particle number and flux density on the gas feeding of the plasma source. Helical field corresponds to R_{mean}=1.35. From left to right, from top to bottom: (a) number of particles in the entrance tank; plasma flux (b) at the entrance of the transport section; (c) in the middle of the transport section; (d) on the upstream and downstream sides of the Mach probe.

The electron temperature does not depend on the mean corrugation ratio and guiding magnetic field (Fig. 7 a) and decreases slowly with the rise of the plasma density (Fig. 7 c). At the same time, the potential drop between the center and the periphery of the plasma drops significantly with the increase of the corrugation ratio, increase of the plasma density and decrease of the guide magnetic field (Fig. 7 b,d). All of these processes presumably lead to the increase of the radial transport.

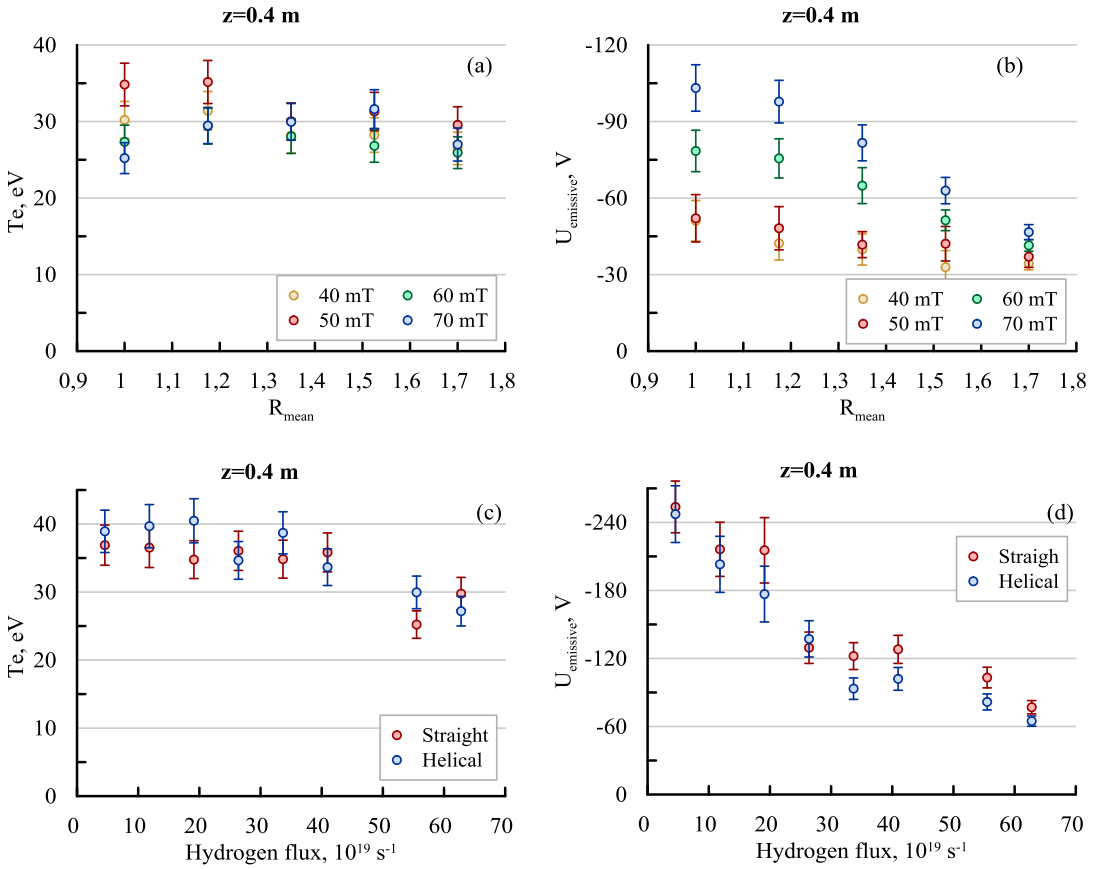

FIG. 7. From left to right, from top to bottom: (a, c) dependence of the electron temperature on the helical magnetic field amplitude and the gas feeding of the plasma source, correspondingly; (b, d) dependence of the plasma potential on the helical magnetic field amplitude and the gas feeding of the plasma source, correspondingly.

4. PARTICLE BALANCE

If the density inside the entrance tank exceeds $n \sim 10^{18}$ m^{-3} the losses are gas dynamic. They are balanced with the new ions from the plasma source and the return flux generated by the transport section. The plasma is being neutralized on the walls and the neutral gas is pumped out. The particle balance inside the confinement region can be described in the following form:

$$nvS_0\left(\frac{1}{R_1}+\frac{1}{R_2}\right)=F_{feed}+F_{return}\ ,$$

where n and v are the density and the velocity of the ions in the entrance tank, S_0 is the cross-section of the plasma in the weakest magnetic field, $R_1 = 8$ and $R_2 = 3$ are the simple mirror ratio of the weakest magnetic field to the plasma source field and to the guide magnetic field of the cross-section, F_{feed} is the flux of the plasma source feeding and F_{return} is the return flux from the transport section. Integration of the data obtained by the double probes provides the sum of the fluxes $nvS_0 + F_{return}$. This value can be compared with the theory, but it has the practical meaning only outside of the transport section and at its end, where the return flux should be negligible. Their difference at the inlet of the transport section can be used to define the effective mirror ratio:

$$F_{feed}=\frac{nvS_0}{R_1}+\left(\frac{nvS_0}{R_2}-F_{return}\right)=nvS_0\left(\frac{1}{R_1}+\frac{1}{R_{eff}}\right)$$

Direct calculation of the R_{eff} from the experimental data is obstruct because the difference between F_{feed} and gas dynamic losses towards the plasma source is close to zero. The lower estimate may be evaluated, giving $R_{eff} > 5$ at $R_{mean} = 1.35$, $R_{eff} > 8$ at $R_{mean} = 1.52$ and $R_{eff} > 10$ at $R_{mean} = 1.7$.

The flux towards the plasma source with the local density excessing the density of the flux in the forward direction was observed directly. This flux is generated close to the plasma axis. Its occurrence takes place jointly with the reduction of the width of the forward flux. Both of these facts stand in the qualitative agreement with the theoretical model. This return flux in model should consist of the trapped particles and therefore have the mean velocity comparable to the axial velocity of the multiple mirror movement. Such flux by itself can be a source of the energy for the microinstabilities which lead to the anomalous scattering. Presence of the anomalous scattering is required to obtain high efficiency of the multiple mirror confinement if the mean free path with respect to Coulomb scattering is higher than the period of the magnetic corrugation. Linear dependence of the experimentally measured particle fluxes on the plasma density and higher level of the noise in the probe data in the helical configuration may be the indirect evidences of this process, but the question of the microinstability level requires further investigations.

5. CONCLUSION

The experimental results on the plasma flow in the helical mirror were obtained. High rotation velocity and high mean corrugation ratio made it possible to observe the effect of the dynamic multiple mirror scheme clearly. With high corrugation ratio the plasma density between the simple mirror and the helical one was increased by the factor of 1.6 compared to the straight magnetic system. The integral flux from the transport section drops below the detectable level. The effective mirror ratio of the helical section was $R_{eff} > 10$.

Dependencies of the plasma flux in different positions along the helical section on the mean corrugation ratio and the plasma density were measured. Increase in the corrugation ratio suppresses the flux from the plasma source and increases the flux in the opposite direction. At high corrugation ratio the flux direction is different on the axis and on the periphery of the plasma. All fluxes scale linearly on the plasma density, even if the mean free path of the ion with respect to the Coulomb scattering is 4–8 times higher than the period of the corrugation.

ACKNOWLEDGEMENTS

This work was supported by the Russian Science Foundation (project No. 18-72-10080). The results related to this project are discussed in chapters 2, 3, 5. Parts of the study related to the particle balance (chapter 4) were supported by grant of President of Russian Federation SP-1242.2021.2. Maintenance of the SMOLA device is supported by the Ministry of Science and Higher Education of the Russian Federation.

REFERENCES

[1] BEKLEMISHEV, A., et al., Novosibirsk project of gas-dynamic multiple-mirror trap, Fusion Sci. Technol. **63** 1T (2013) 46.

[2] POSTUPAEV, V. V., et al. The GOL-NB program: further steps in multiple-mirror confinement research, Nuclear Fusion **57** (2017) 036012.

[3] BEKLEMISHEV, A., Helicoidal system for axial plasma pumping in linear traps, Fusion Sci. Technol. **63** 1T (2013) 355.

[4] BE'ERY, I., et al, Plasma confinement by moving multiple mirrors, Plasma Phys. Control. Fusion **60** (2018) 115004.

[5] BEKLEMISHEV, A., Radial and axial transport in trap sections with helical corrugation, AIP Conference Proceedings **1771** (2016) 040006.

[6] CHERNOSHTANOV, I.S., AYUPOV, D. A. Collisionless particle dynamics in trap sections with helical corrugation, Phys. of Plasmas **28** (2021) 032502.

[7] POSTUPAEV, V. V., et al, Helical mirrors for active plasma flow suppression in linear magnetic traps, Fusion Eng. Design **106** (2016) 29.

[8] SUDNIKOV, A. V., et al., SMOLA device for helical mirror concept exploration, Fusion Eng. Design. **122** (2017) 85.

[9] SUDNIKOV, A.V. et al., First experimental campaign on SMOLA Helical Mirror, Plasma and Fusion Research, **14** (2019) 2402023

[10] SUDNIKOV, A.V., et al., Preliminary experimental scaling of the helical mirror confinement effectiveness, J. Plasma Phys. **86** 5 (2020) 905860515.

[11] IVANOV, I. A., et al, Long-pulse plasma source for SMOLA helical mirror, J. Plasma Phys. **87** 2 (2021) 845870201.

[12] INZHEVATKINA, A.A., et al, Investigation of the plasma rotation in SMOLA helical mirror. Rev. of Plasma Phys. In press (2021).